CRYSTAL GROWTH & DESIGN
Article
2010, Vol. 10
1233–1236

DOI: 10.1021/cg9012284

Morphological Control of Single Crystalline Co_3O_4 Polyhedrons: Selective and Nonselective Growth of Crystal Planes Directed by Differently Charged Surfactants and Solvents

Jinhu Yang[†,‡] and Takehiko Sasaki*[,†]

[†]*Department of Complexity Science and Engineering, School of Frontier Sciences,*
The University of Tokyo, 5-1-5, Kashiwanoha, Kashiwa, Chiba 277-8561, Japan, and [‡]*The Institute for*
Advanced Materials & Nano Biomedicine, Tongji University, Shanghai 200092, China

Received October 6, 2009; Revised Manuscript Received January 29, 2010

ABSTRACT: Single-crystalline Co_3O_4 crystals such as spheres, nanocubes, and rhombododecahedrons were obtained hydrothermally by employing differently charged surfactants and solvents. On the basis of calculations (charge density, atom density, and dipolar moment) on involved charged crystal planes of {100} for the cubes and {110} for the rhombododecahedrons, we proposed that the specific interactions between changed capping agents and crystal planes of Co_3O_4 led to the selective formation of cubes with {100} orientation and rhombododecahedrons with {110} orientation, respectively. It was also found that the intrinsic structure of charged planes affected possibly not only the crystallization processes and final morphologies of Co_3O_4 crystals but also the assembly behaviors of Co_3O_4 particles. Being in a typical spinel structure, the crystallization habits of Co_3O_4 crystals based on intrinsic structure directed by capping agents are possibly extended to other crystal systems in a similar structure, to get an optimized synthetic strategy and product, which, as well, is helpful for understanding the interactions on the organic−inorganic interfaces in depth.

Introduction

Controlling the size, shape, and structure of inorganic materials is of fundamental significance in modern science and engineering, because both the intrinsic properties of materials and performances of these material-based devices for applications are highly dependent on the morphology and structure of the materials themselves.[1−5] As a prevailing and effective means, the wet chemical method coupled with organic additives such as polymers, surfactants, and other small molecules has been employed successfully for controlled synthesis of inorganic crystals, where organic additives worked as templates or capping agents through interactions with crystals between the "soft−hard" interfaces to vary the surface energy of crystal planes, thus realizing the growth control over the corresponding crystal planes.[6] For example, some kinds of interaction modes such as structure match,[7] electric charge effect,[8] etc. between the organic molecules and the specific planes of crystals have been investigated. Nevertheless, these interaction modes are often case-dependent, due to both the selection of organic molecules and the inorganic crystal structures involved, and the exact interaction mechanism still remains unsolved. Herein, we adopted Co_3O_4, whose structure is a typical spinel system.

Co_3O_4 is an active material with wide applications[9−13] and has attracted much attention to the shape-controlled synthesis by various routes such as wet chemical methods, nanocasting, thermal oxidation, mechanochemical reactions, etc.[13−24] Among these, the wet chemical methods are the most prevalent for the shape control of Co_3O_4 crystals. However, there are still limited investigations on the interfacial interaction mechanisms between organic capping molecules and Co_3O_4 crystals that probably determine the final morphologies of Co_3O_4 crystals in solution synthesis processes. Therefore, in the present study we demonstrated the selective and nonselective growth of crystal planes of Co_3O_4 directed by the differently charged surfactants/solvents and the morphology control of Co_3O_4 crystals with spheres, cubes, and especially rhombododecahedrons that is synthesized for the first time as Co_3O_4 phase. These results are also of fundamental importance for understanding the interaction between specific crystal planes and the capping agents. As is well-known, ZnO crystals favor the preferential growth along the ⟨0001⟩ direction[25] and nanobelts bounded by {0001} planes self-coil into nanorings,[26] due to the charged {0001} planes possessing a separate Zn^{2+} layer and O^{2-} layer. In this regard, our systematic studies are beneficial for not only recognizing the specific organic−inorganic interfacial interactions based on the charged crystal planes but also the controlled synthesis and self-assembly behaviors of Co_3O_4 and other compounds with similar crystal structures.

Experimental Section

In a typical synthesis of Co_3O_4 rhombododecahedrons, 0.003 g of cobalt chloride were added with slight stirring into a 100 mL Teflon autoclave containing 9 mL mixture of *N*,*N*- dimethylformamide (DMF), acetonitrile, and distilled water at 1:1:1 (v/v), giving a final pink solution. Subsequently, after 2 mL of 30% H_2O_2 was added, the autoclave was heated at 150 °C in an oven for 20 h, giving a black precipitate. For the synthesis of Co_3O_4 cubes, hexadecyltrimethylammonium chloride (CTAC) or sodium dodecyl sulfate (SDS) at certain concentrations were used before the addition of cobalt chloride; other conditions were the same as for Co_3O_4 rhombododecahedrons. In the case of the preparation for Co_3O_4 spheres, all procedures were similar to that of cube synthesis except nonionic surfactant of Triton X-100 (e.g., 8 mM) was used instead of ionic surfactants of CTAC or SDS. The products were collected with the centrifuge method, washed with water, dried in air, and characterized by scanning electron microscopy (SEM, JSM-5510LV, 10 kV), transmission electron microscopy (TEM, JEOL JEM-2010F, 200 kV), and powder X-ray diffraction (XRD, Rigaku RINT-2500 V, Cu Kα).

---

*Corresponding author. Tel/fax: +81-4-7136-3910; e-mail: takehiko@k.u-tokyo.ac.jp.

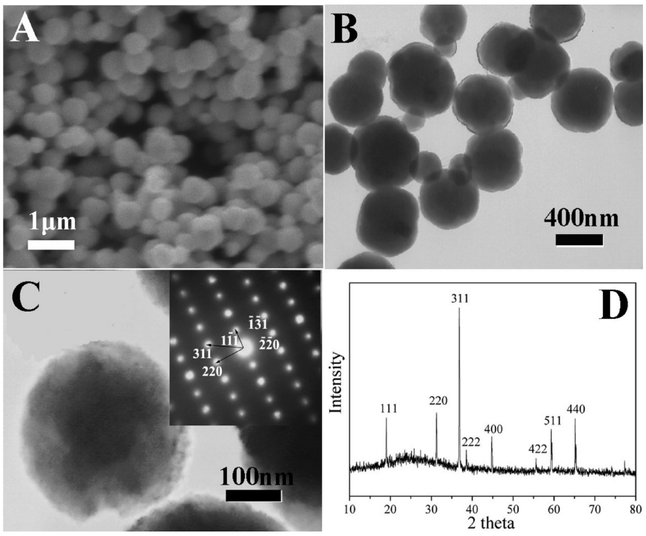

Figure 1. SEM (A), TEM images (B, C), and XRD pattern (D) of Co_3O_4 single-crystal spheres formed in the presence of 8 mM Triton X-100. Inset in C is the ED pattern corresponding to the Co_3O_4 sphere centered in C.

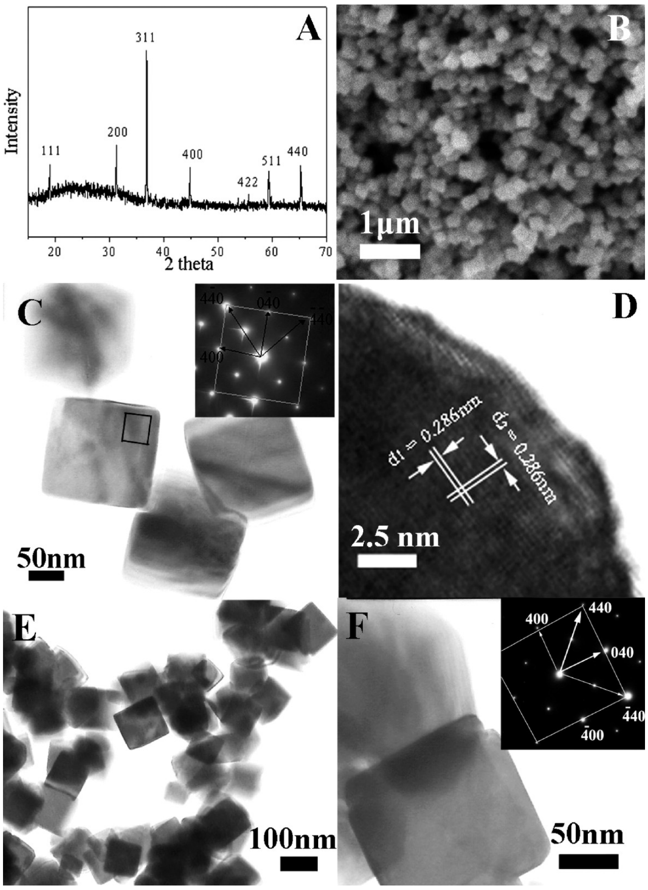

Figure 2. XRD (A), SEM (B), and TEM images (C−F) of Co_3O_4 nanocubes formed in the presence of CTAC (A−D) and SDS (E, F), respectively. Insets in C and F correspond to the Co_3O_4 nanocubes in C (labeled) and F, respectively. Both CTAC and SDS concentrations are 4 mM.

Results and Discussion

The Co_3O_4 spheres were prepared in Triton X-100 instead of ionic surfactants. As shown in Figure 1, both SEM and TEM images present a clearly sphere-like shape of Co_3O_4 crystals with 8 mM Triton X-100. These Co_3O_4 spheres possess a relatively uniform size of 400 nm except minor spheres with a smaller size of ca. 100 nm (Figure 1B). The electron diffraction (ED) pattern (inset in Figure 1C) of the centered individual sphere exhibits the sharp spots corresponding well to the crystal plane reflections of Co_3O_4 crystals of cubic symmetry, indicating a single-crystal structure. The Co_3O_4 phase of these spheres were also confirmed by XRD (JPCDS: 43-1003) in Figure 1D, which agrees with the ED pattern in Figure 1C.

In contrast, the Co_3O_4 nanocubes were synthesized in the presence of ionic surfactants, regardless of charge types. As shown in Figure 2A, the XRD pattern of the product formed in CTAC (4 mM) provides a Co_3O_4 phase of the nanocubes. SEM image in Figure 2B shows that the Co_3O_4 nanocubes occupy an average diameter of ∼150 nm and stack into a dense layer on substrate. In Figure 2C, several Co_3O_4 nanocubes at different tilt angles against substrate were selected for TEM observation, which gives distinct cubic characteristics. Moreover, the ED pattern (inset of Figure 2C) corresponding to the squared area of a vertically standing Co_3O_4 nanocube exhibits sets of bright reflections with the spacing corresponding to (220) and (400) planes of cubic Co_3O_4 crystals, revealing the Co_3O_4 nanocube is a single crystal and the diffracted planes are {100} planes. In addition, the high-resolution TEM image in the same squared area displays continuous fringes and the two sets of orthogonal lattices with equivalent *d*-spacing of 0.286 nm corresponding to {220} planes of Co_3O_4 crystal, which reflects that the observed face is bound by {100} planes. Similarly, Co_3O_4 nanocubes with a diameter of ∼120 nm were also produced in the presence of anionic surfactant SDS instead of CTAC, as evidenced by the TEM observations and electron diffraction (ED) patterns of individual Co_3O_4 nanocubes (Figure 2E,F). These results demonstrate that the Co_3O_4 nanocubes surrounded by {100} planes were produced in either kind of oppositely charged surfactant of CTAC and SDS. In addition, the effect of surfactant concentrations was examined, for example, increasing the currently employed concentration by three times; however, neither the nonionic nor ionic surfactants had a remarkable effect on the morphologies of Co_3O_4 crystals, indicating the adsorptions were already saturated.

To clarify the effect of surfactants, the synthesis was further conducted in the absence of surfactants, that is, in the solution of a polar DMF−acetonitrile mixture, resulting in the formation of Co_3O_4 rhombododecahedrons, that is synthesized for the first time as Co_3O_4 polyhedrons other than cubes. The Co_3O_4 rhombododecahedrons synthesized exhibit hexagonal outlines with approximately 200 nm in average diameter between two parallel faces, as observed in Figure 3A,B. More solid structural information was given from TEM characterizations. The ED pattern (inset in Figure 3C) corresponding to the squared area of an individual Co_3O_4 rhombododecahedron show two sets of bright diffraction spots, which can be indexed well as {200} and {111} planes with corresponding *d*-spacing of 4.04 and 4.67 nm, respectively, revealing a diffraction of {110} planes. This result was supported as well by the high-resolution TEM examination from the same area of the Co_3O_4 rhombododecahedron labeled (Figure 3D). Actually, for the arbitrarily selected Co_3O_4 rhombododecahedrons, the diffractions of {110} planes occupied most majorities in the ED observations except that diffractions from other planes, such as {111} planes (Figure 3E), through appropriate tilting manipulations. This accords pretty well

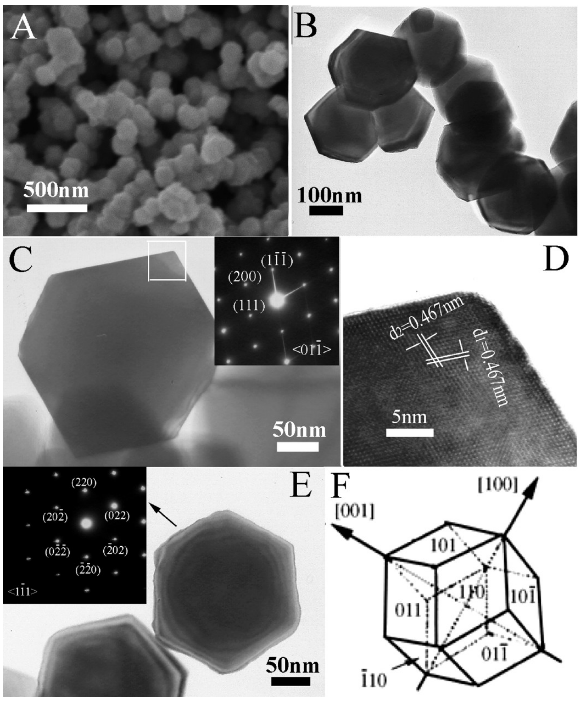

Figure 3. SEM (A) and TEM (B–E) images and index (F) of Co_3O_4 rhombododecanhedrons formed in the absence of surfactants. D is a high-resolution TEM image corresponding to the square area of the Co_3O_4 rhombododecahedron in C. Insets in C and E are ED patterns corresponding to Co_3O_4 rhombododecahedrons in C and E, respectively.

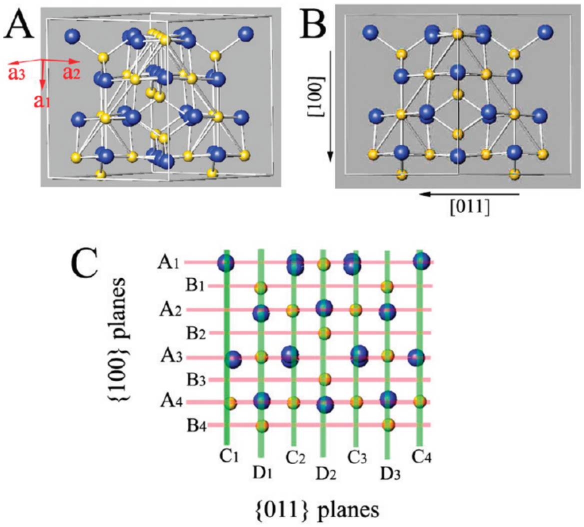

Figure 4. Overview (A), particular view (B) through the $[0\bar{1}\bar{1}]$ direction of the crystal structure of Co_3O_4 crystal (unit cell) and the atoms of unit cell in B divided along the {100} and {011} planes, respectively (C). Bigger blue spheres: O atoms; smaller yellow spheres: Co atoms.

with the typical symmetry of the rhombododecahedral shape, because a rhombododecahedron is surrounded by 12 equivalent {110} faces (Figure 3F), and one of 12 {110} faces parallel to the substrate (Cu grid) is the only stable state in energy for a standing rhombododecahedron, which inevitably causes the diffractions of {110} planes as we observed.

In order to clarify the mechanism responsible for the crystal-plane modulation of Co_3O_4 polyhedrons under the different conditions, the crystal structure of Co_3O_4 crystal, especially the cases of {100} and {110} planes, was analyzed. Figure 4A presents a typical crystal structure of the Co_3O_4 crystal (unit cell), where eight molecular Co_3O_4 were contained. For the convenience of comprehension, the crystal structure was displayed perpendicular to the $[0\bar{1}\bar{1}]$ direction (Figure 4B) and then the atoms in the unit cell were divided into $A_{1\to4}$/$B_{1\to4}$ layers along the {100} planes and $C_{1\to4}$/$D_{1\to4}$ layers along the {011} planes (Figure 4C), respectively (see Supporting Information, S1). On the basis of the coordinates of Co and O atoms in the unit cell of Co_3O_4 crystal, the valences of O atoms in the unit cell are adopted as 2−, while the valences of Co atoms on A and B layers are adopted as 3+ and 2+, respectively. According to the divisions, the charge densities and atom densities corresponding to the A–D layers were calculated. The charge density of slabs can be calculated ±0.061 e·Å^{-2} for {100} and $\pm$ 0.043 e·Å^{-2} for {110} planes, respectively (See Supporting Information S2-1). Both the {100} and {110} planes are polar. We can consider the pair of slabs with the opposite charge for both orientations, of which accumulation yielded crystal growth along either orientation. We believe that the charging property and charging extent of crystal planes probably have a remarkable influence on both crystallization and assembly processes of crystals. For example, it was observed that the Co_3O_4 polyhedrons synthesized in our system (Figures 1 and 2) or nanocubes reported elsewhere[19,20] are apt to be stack or tiered, which should be ascribed to the strongly electrostatic attraction between oppositely charged crystal planes, although sometimes it was rationally attributed to surfactant interlayers between nanocubes.[20]

Here, based on the results and analysis above, a mechanism stressing electric charge effect between the differently charged capping agents and charged crystal planes is tentatively proposed to account for the crystal orientations of Co_3O_4 polyhedrons (Scheme 1). Briefly, when the nonionic Triton X-100 was used, the neutral chains cause the nonselective adsorption on the crystal surfaces, leading to the formation of the Co_3O_4 spheres without specific crystal-plane orientations. However, in the presence of ionic surfactants of CTAC or SDS, the charged R_4N^+ and SO_4^{2-} groups of the surfactants preferentially adsorbed on highly charged {100} planes rather than relatively less charged {110} due to more pronounced electrostatic attractions between the surfactants and {100} planes of Co_3O_4 crystals, leading to the growth inhibition of {100} planes and final generation of the Co_3O_4 nanocubes. In fact, highly charged {100} planes with lower atom density (calculations, Supporting Information, S2-2) are more unstable than less charged {110} planes if exposed without protection of strong capping agents like CTAC or SDS. Therefore, we consider this is a system-energy-minimizing process, and the strong interactions between CTAC or SDS molecules and {100} planes caused the formation of the Co_3O_4 nanocubes. For the polar molecules of DMF and acetonitrile, which are neutral and weak capping agents as compared with CTAC or SDS, they just exert weaker interactions with {100} planes of Co_3O_4 crystals, which could not compensate the system energy increase accompanied by the formation of {100} planes relative to {110} planes, and thus adsorbed on the relatively stable {110} planes, producing the Co_3O_4 rhombododecahedrons. Accordingly, the Co_3O_4 rhombododecahedrons were prepared in the mixed solvents DMF and acetonitrile without ionic surfactants. In a word, the strong enough electric charge effect is a key factor for the formation of nanocubes with highly charged {100} planes of

Scheme 1. Possible Mechanism for Co_3O_4 Polyhedrons Synthesized in the Presence of Differently Charged Surfactants and Solvents

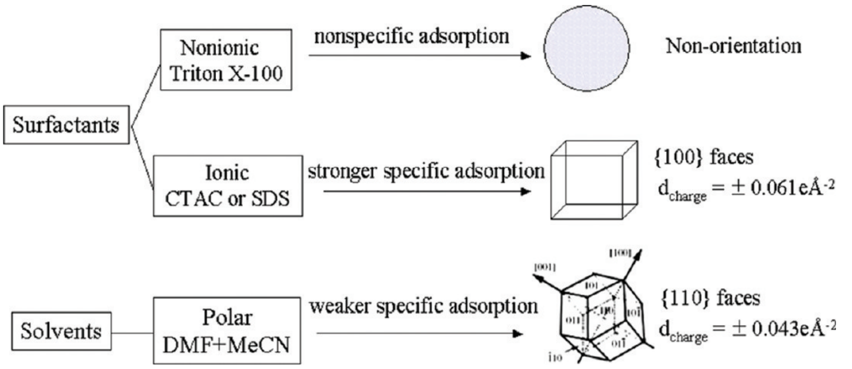

Co_3O_4 crystals. Though our proposed mechanism does not include the knowledge of the exact atomic structure of the exterior surface of crystals, which would be necessary for the complete theoretical comprehension, it is applicable to the previous reports on the Co_3O_4 nanocube synthesis, where the nanocubes were synthesized in the presence of highly charged capping agents, such as SDBS, anions derived from Tween-85 or $NaNO_3$ at high concentration.[19,20]

Conclusions

In conclusion, the Co_3O_4 crystals with various shapes involving spheres, nanocubes, and rhombododecahedrons have been synthesized hydrothermally in the presence of differently charged surfactants/solvents. The realization of successfully modulating the Co_3O_4 polyhedrons with differently crystal-plane orientation relies probably on the electric charge effect between the charged capping agents and the charged planes of Co_3O_4 crystals. The results are associated with the relationship between the crystallization habit and the intrinsic crystal structure of Co_3O_4 crystals, and in principle, are expected to be applicable to other systems with similar crystal structures besides Co_3O_4 crystals, which would result in a better understanding the specific interactions of organic and inorganic phases between "soft−hard" interfaces.

Acknowledgment. J.Y. gratefully acknowledges the financial support from the Japan Society for the Promotion of Science (ID: 18·06080), the Research Fund for the Doctoral Program of Higher Education of China (20090072120013), and the Program for Young Excellent Talents in Tongji University (4340219003). T.S. acknowledges the support by a Grant-in-Aid for Scientific Research (No. 19550008) from JSPS. The present study was also supported in part by the Ministry of Education, Culture, Sports, Science and Technology (MEXT) of Japan (No. 20031008, Grant-in-Aid for Scientific Research in Priority Area "Science of Ionic Liquids). The TEM measurement was performed at the Institute for Solid State Physics, the University of Tokyo.

Supporting Information Available: The structure information, the charge density, atom density, and dipolar moment calculations of Co_3O_4 crystal. This material is available free of charge via the Internet at http://pubs.acs.org.

References

(1) Burda, C.; Chen, X.; Narayanan, R.; El-Sayed, M. A. *Chem. Rev.* **2005**, *105*, 1025.
(2) Yin, Y.; Alivisatos, A. P. *Nature* **2005**, *437*, 664.
(3) Cölfen, H.; Mann, S. *Angew. Chem., Int. Ed.* **2003**, *42*, 2350.
(4) Jin, R.; Cao, Y.; Mirkin, C. A.; Kelly, K. L.; Schatz, G. C.; Zheng, J. G. *Science* **2001**, *294*, 1901.
(5) Xiong, Y. J.; Xia, Y. N. *Adv. Mater.* **2007**, *19*, 3385.
(6) (a) Sone, E. D.; Zubarev, E. R.; Stupp, S. I. *Angew. Chem., Int. Ed.* **2002**, *41*, 1705. (b) Antonietti, M. *Curr. Opin. Colloid Interface Sci.* **2001**, *6*, 244. (c) Yu, S. H.; Cölfen, H. *J. Mater. Chem.* **2004**, *14*, 2124.
(7) (a) Yu, S. H.; Cölfen, H.; Mastai, Y. *J. Nanosci. Nanotechnol.* **2004**, *4*, 291. (b) Lochhead, M. J.; Letellier, S. R.; Vogel, V. *J. Phys. Chem. B* **1997**, *101*, 10821.
(8) (a) Volkmer, D.; Fricke, M.; Agena, C.; Mattay, J. *J. Mater. Chem.* **2004**, *14*, 2249. (b) Zhao, N. N.; Qi, L. M. *Adv. Mater.* **2006**, *18*, 359. (c) Ouyang, J. M.; Deng, S. P. *Dalton Transact.* **2003**, *14*, 2846.
(9) Cao, A. M.; Hu, J. S.; Liang, H. P.; Song, W. G.; Wan, L. J.; He, X. L.; Gao, X. G.; Xia, S. H. *J. Phys. Chem. B* **2006**, *110*, 15858.
(10) Radwan, N. R. E.; Mokhtar, M.; El-Shobaky, G. A. *Appl. Catal. A: General* **2003**, *241*, 77.
(11) Maruyama, T.; Arai, S. *J. Electrochem. Soc.* **1996**, *143*, 1383.
(12) Avila, A. G.; Barrera, E. C.; Huerta, L. A.; Muhl, S. *Sol. Energy Mater. Sol. Cells* **2004**, *82*, 269.
(13) (a) Poizot, P.; Laruelle, S.; Grugeon, S.; Dupont, L.; Tarascon, J. M. *Nature* **2000**, *407*, 496. (b) Li, W. Y.; Xu, L. N.; Chen, J. *Adv. Funct. Mater.* **2005**, *15*, 851.
(14) Li, Y. G.; Tan, B.; Wu, Y. Y. *J. Am. Chem. Soc.* **2006**, *128*, 14258.
(15) Shi, X. Y.; Han, S. B.; Sanedrin, R. J.; Zhou, F. M.; Selke, M. *Chem. Mater.* **2002**, *14*, 1897.
(16) (a) Yoshikawa, H.; Hayashida, K.; Kozuka, Y.; Horiguchi, A.; Awaga, K.; Bandow, S.; Iijima, S. *Appl. Phys. Lett.* **2004**, *85*, 5288. (b) Hou, Y.; Kondoh, H.; Shimojo, M.; Kogure, T.; Ohta, T. *J. Phys. Chem. B* **2005**, *109*, 19094.
(17) (a) Wang, Y.; Yang, C. M.; Schmidt, W.; Spliethoff, B.; Bill, E.; Schuth, F. *Adv. Mater.* **2005**, *17*, 53. (b) Xiong, S. L.; Yuan, C. Z.; Zhang, M. F.; Xi, B. J.; Qian, Y. T. *Chem.—Eur. J.* **2009**, *15*, 5320.
(18) Yue, W. B.; Hill, A. H.; Harrison, A.; Zhou, W. Z. *Chem. Commun.* **2007**, 2518.
(19) He, T.; Chen, D. R.; Jiao, X. L.; Wang, Y. L. *Adv. Mater.* **2006**, *18*, 1078.
(20) (a) Feng, J.; Zeng, H. C. *Chem. Mater.* **2003**, *15*, 2829. (b) Xu, R.; Zeng, H. C. *Langmuir* **2004**, *20*, 9780.
(21) Shao, Y. Z.; Sun, J.; Gao, L. *J. Phys. Chem. C* **2009**, *113*, 6566.
(22) Garcia-Pacheco, G.; Cabanas-Moreno, J. G.; Yee-Madeira, H.; Cruz-Gandarilla, F. *Nanotechnology* **2006**, *17*, 2528.
(23) He, L.; Li, Z. C.; Zhang, Z. J. *Nanotechnology* **2008**, *19*, 155606.
(24) Salabas, E. L.; Rumplecker, A.; Kleitz, F.; Radu, F.; Schuth, F. *Nano Lett.* **2006**, *6*, 2977.
(25) Yu, H. D.; Zhang, Z. P.; Han, M. Y.; Hao, X. T.; Zhu, F. R. *J. Am. Chem. Soc.* **2005**, *127*, 2378.
(26) Kong, X. Y.; Ding, Y.; Yang, R.; Wang, Z. L. *Science* **2004**, *303*, 1348.